Biochimica et Biophysica Acta, 1146 (1993) 219–228

BBAMEM 75905

Influence of lipid lateral distribution on the surface charge response of the phosphatidylcholine headgroup as detected using ^{2}H nuclear magnetic resonance

Francesca M. Marassi, Selma Djukic and Peter M. Macdonald

Department of Chemistry and Erindale College, University of Toronto, Toronto, Ontario (Canada)

(Received 28 August 1992)
(Revised manuscript received 23 November 1992)

Key words: NMR, ^{2}H-; Phosphatidylcholine; Surface charge; Lipid lateral distribution

The effect of lipid lateral distribution on the surface charge response of the phosphatidylcholine headgroup, in bilayers composed of binary mixtures of 1-palmitoyl-2-oleoyl-*sn*-glycero-3-phosphocholine (POPC) and 1,2-dimyristoyl-*sn*-glycero-3-phosphate (DMPA), was investigated by monitoring the deuterium nuclear magnetic resonance (^{2}H-NMR) spectrum of choline-deuterated phosphatidylcholine as a function of temperature and DMPA concentration. Addition of DMPA at temperatures corresponding to fully liquid-crystalline membranes caused a progressive increase (decrease) in the ^{2}H-NMR quadrupole splitting from POPC-α-d_2 (POPC-β-d_2), in agreement with the known response of phosphatidylcholine to negative membrane surface charge (Seelig, J., Macdonald, P.M. and Scherer, P.G. (1987) Biochemistry 26, 7535–7541). Lateral phase separation of DMPA-rich domains was induced in these mixtures by lowering the temperature in the range from 60°C to −15°C, and was accompanied by a reversal of the original effects of DMPA on the quadrupole splitting. Analysis of the ^{2}H-NMR spectral response allows one to generate a temperature/composition phase diagram for the POPC/DMPA system. We conclude that ^{2}H-NMR of headgroup-deuterated phosphatidylcholine can be employed to sense and to quantify inhomogeneities in the lateral distribution of charged membrane components.

Introduction

^{2}H-NMR of headgroup-deuterated phosphatidylcholine has proved to be an enormously useful means of detecting the charge at the surface of lipid bilayer membranes [1–5]. Surface charge appears to induce a conformational change in the phosphocholine headgroup, which is then reflected in the ^{2}H-NMR spectrum. This so-called 'molecular voltmeter' has been employed to monitor the surface charge effects of a wide range of biologically interesting compounds including aqueous ions [2,6–8], hydrophobic ions [9], local anaesthetics [10,11], charged proteins [12,13], charged peptides [3], and charged amphiphiles [4].

To date, all such studies have been carried out under conditions of complete miscibility of the membrane components. In this case, the membrane surface charge may be considered to be uniformly smeared in the plane of the bilayer [14,15], and the ^{2}H-NMR results reflect a homogeneous charge distribution. However, it is clear that within biological membranes there can exist long-lived domains of distinct composition, supporting specific biological functions. For example, certain lipid components of biological membranes exist close to the gel state at physiological temperatures, and their lateral phase separation may play a role in regulating those biological functions sensitive to membrane fluidity and compressibility [16–19]. As well, certain membrane proteins tend to aggregate, forming domains enriched in those components which stabilize or are stabilized by such an environment [20]. The role of surface electrostatics in promoting such distributional heterogeneities, and their effects upon local surface charge, will be considerable. It is uncertain, however, how the 'molecular voltmeter'

Correspondence to: P.M. Macdonald, Department of Chemistry and Erindale College, University of Toronto, Toronto, Ontario, Canada, M5S 1A1.

Abbreviations: NMR, nuclear magnetic resonance; DSC, differential scanning calorimetry; TLC, thin-layer chromatography; ^{2}H, deuterium; ^{1}H, proton; $\Delta\nu$, quadrupole splitting; POPC, 1-palmitoyl-2-oleoyl-*sn*-glycero-3-phosphocholine; POPA, 1-palmitoyl-2-oleoyl-*sn*-glycero-3-phosphate; DMPA, 1,2-dimyristoyl-*sn*-glycero-3-phosphate; Hepes, 4-(2-hydroxyethyl)piperazine-1-ethanesulfonic acid; TPS, 2,3,5-triisopropylbenzenesulfonyl chloride.

will respond in such a situation where the surface charge is no longer smeared uniformly over the bilayer plane.

The goal of this study is to describe the response of the 'molecular voltmeter' to a nonuniform surface charge distribution. Our model system consists of binary mixtures of 1-palmitoyl-2-oleoyl-*sn*-glycero-3-phosphocholine (POPC) with 1,2-dimyristoyl-*sn*-glycero-3-phosphate (DMPA). DMPA, by virtue of its negative charge, will induce a characteristic change in the ^{2}H-NMR quadrupole splitting measured from headgroup-deuterated POPC. By virtue of its high gel/liquid-crystalline phase transition temperature (52°C) [22,23] relative to that of POPC (−5°C) [21], the POPC/DMPA mixtures may be expected to exhibit lateral phase separation at temperatures intermediate between those of the pure components. In the following we describe the impact of the resulting nonuniform charge distribution on the ^{2}H-NMR spectrum from headgroup-deuterated POPC, and the consequences for the interpretation of the ^{2}H-NMR quadrupole splitting in terms of membrane surface charge.

Materials and Methods

Synthesis of headgroup-deuterated lipids. The structures of the phosphocholine (I) and phosphatidic acid (II) headgroups are shown below. The α and β nomenclature employed for the deuterium-labeled segments of the phosphocholine headgroup is also indicated.

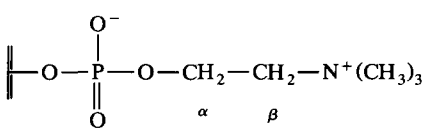

I

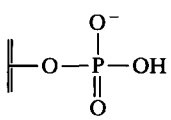

II

Non-deuterated lipids were purchased from Avanti (Alabaster, AL). Choline was selectively deuterated at the α and β segments by a combination of the methods described by Harbisson and Griffin [24] and Aloy and Rabaut [25]. POPC-α-d_2 and POPC-β-d_2 were prepared by coupling 1-palmitoyl-2-oleoyl-*sn*-glycero-3-phosphate (POPA) with choline tetraphenylboron salt, selectively deuterated at the α or β segment, using 2,4,6-triisopropylbenzenesulfonyl chloride (TPS) as the condensing agent [26]. The choline-deuterated phosphatidylcholines were purified by chromatography on silica gel and CM-52 as described by Comfurius and Zwaal [27], and their purity was checked by TLC, ^{1}H-NMR, and DSC.

Sample preparation. Samples for ^{2}H-NMR studies were prepared as follows. 5 to 10 mg of deuterated POPC, plus the desired amount of DMPA, all in chloroform solution, were mixed by vortexing. The solvent was removed under a stream of nitrogen, followed by high vacuum, and the dried lipids were dispersed in excess deuterium-depleted aqueous buffer (150 mM NaCl, 10 mM Hepes, pH 7) by vortexing and warming to 60°C in order to ensure homogeneous mixing. The dispersions were then centrifuged at $13\,000 \times g$ and the pellets were taken for NMR measurement. The purity of the samples was checked by TLC before and after the NMR experiments.

NMR measurements. ^{2}H-NMR spectra were recorded on a Chemagnetics CMX300 NMR spectrometer operating at 45.98 MHz, equipped with a temperature control unit. The quadrupole echo technique [28] was employed, using quadrature detection with complete phase cycling of the pulse pairs [29], and a 90° pulse length of 2.0 μs, an interpulse delay of 40 μs, a recycle delay of 250 ms, a spectral width of 100 kHz, and a data size of 2K. Prior to the NMR experiments the samples were equilibrated at 60°C inside the NMR probe for about 30 minutes. Spectra were recorded at 5 C° intervals in the temperature range from 60°C to −15°C, and the temperature was controlled to within 0.1 C°. Between each interval the temperature was varied at a rate of about 0.25 C°/min, and the samples were equilibrated at each temperature for at least 30 min.

Differential scanning calorimetry. The gel/liquid-crystalline phase transition thermograms were measured using a Perkin-Elmer DSC7 differential scanning calorimeter operating at a scan rate of between 3 and 7 C°/min. Transition exotherms were obtained by cooling from 60°C to −30°C, while endotherms were obtained by heating from −30°C to 60°C. The samples were prepared from nondeuterated lipids as described above except that the aqueous saline buffer contained 50% ethylene glycol. The presence of ethylene glycol suppresses the intense solid/liquid phase transition endotherm from water which would otherwise obscure the relatively weak gel/liquid-crystalline phase transition endotherm of the lipids.

Results

Differential scanning calorimetry

In order to establish that lateral phase separation indeed occurs in the POPC/DMPA system, and to determine the relevant temperatures, we performed differential scanning calorimetry (DSC) measurements on all the POPC/DMPA mixtures. The gel/liquid-crystalline phase transition endotherms obtained by

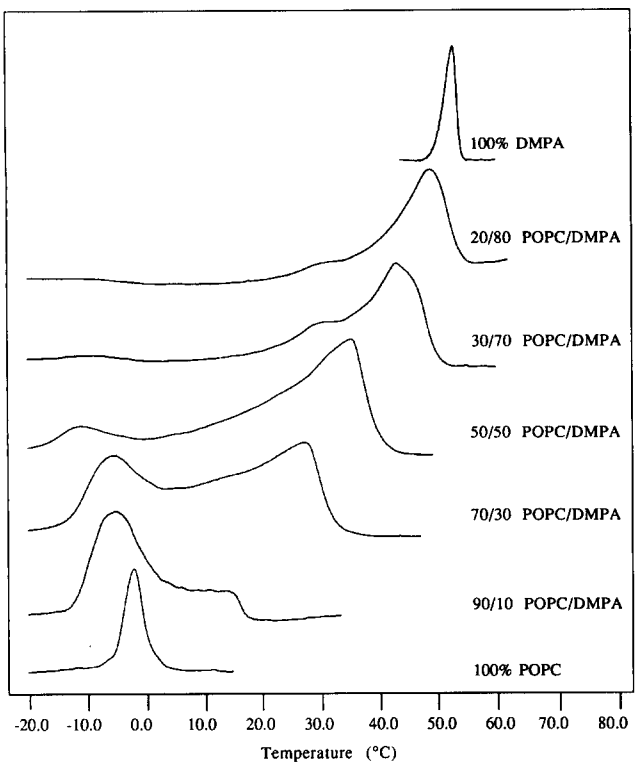

Fig. 1. Differential scanning calorimetry endotherms for membranes containing varying proportions of POPC and DMPA in the indicated molar ratios. Scan rates varied from 3 to 7°C/min.

DSC are shown in Fig. 1 for representative mixtures of POPC with DMPA. For 100% POPC and 100% DMPA the thermotropic phase transition occurs at −5°C and 52°C, respectively, in agreement with previously reported temperatures for these lipids [21–23].

In contrast to the relatively narrow and symmetric endotherms obtained with the pure lipids, all POPC/DMPA mixtures yield broad, asymmetric phase transitions which, in the concentration range from 10 to about 60 mol% DMPA, appear to be composed of two distinct endotherms. With increasing amounts of DMPA the low temperature transition broadens, shifting to slightly lower temperatures and decreasing in size. Simultaneously, the high temperature peak increases in size and shifts to progressively higher temperatures. The presence of distinct endotherms is consistent with the presence of distinct phases, one enriched in POPC, the other enriched in DMPA. The transition exotherms from cooling runs (not shown) coincide with the endotherms from heating runs, and confirm the above observation of two separate DSC peaks. We conclude that lateral phase separation of DMPA-rich domains does indeed occur in these mixtures.

^{2}H-NMR charge response of POPC

Fig. 2 illustrates the changes which occur in the ^{2}H-NMR spectrum of POPC-α-d_2 (a) and POPC-β-d_2 (b) when mixed with increasing proportions of anionic DMPA, under conditions of complete miscibility of the two phospholipids. These spectra were acquired at 60°C, a temperature above the gel/liquid-crystalline phase transition temperatures of all mixtures. The quadrupole splitting ($\Delta\nu$) corresponds to the separation in hertz between the two maxima of the spectrum.

Addition of anionic DMPA to POPC causes the $\Delta\nu$ to increase in the case of POPC-α-d_2, and to decrease in the case of POPC-β-d_2, relative to their values for 100% POPC. Qualitatively, this counterdirectional change for the α versus the β choline segment is the characteristic charge response of the POPC headgroup and, in this case, indicates the presence of a negative surface charge density. Quantitatively, the values of $\Delta\nu$ are in good agreement with previous reports on the effect of anionic amphiphiles, such as dialkyl phosphates [4] and phosphatidylglycerol [5,30]. Therefore, at 60°C POPC appears to experience the full surface charge density expected in the presence of the added amount of anionic DMPA, confirming the expected complete miscibility of DMPA with POPC at this temperature. Furthermore, each ^{2}H-NMR spectrum consists of a single Pake pattern, characterized by a single quadrupole splitting, implying that phosphatidylcholine is reporting on a globally-averaged surface charge. This situation is brought about by the rapid lateral and rotational diffusion of the miscible lipid components, which tends to average out local instantaneous variations in the surface charge environment. The central, sharp, isotropic line seen in the ^{2}H-NMR spectra of mixtures containing higher DMPA concentrations is

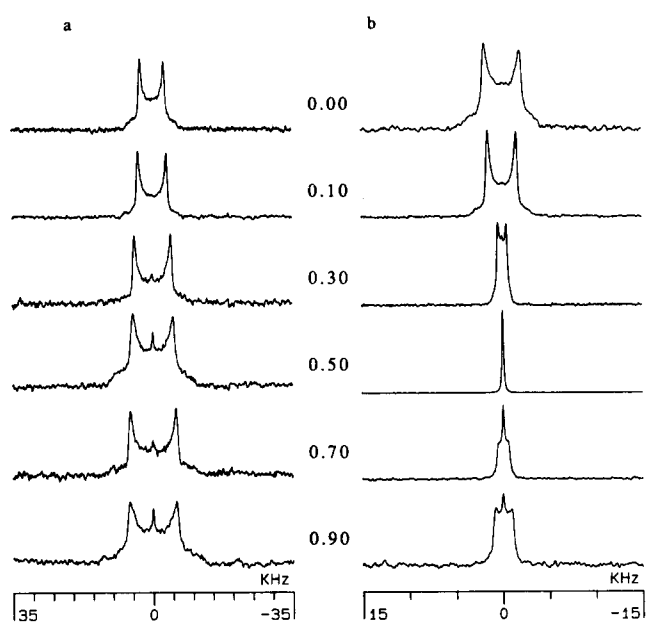

Fig. 2. ^{2}H-NMR spectra at 60°C from headgroup-deuterated POPC in membranes containing the indicated mole fractions of DMPA. Note the difference in the scale for (a) POPC-α-d_2 versus (b) POPC-β-d_2.

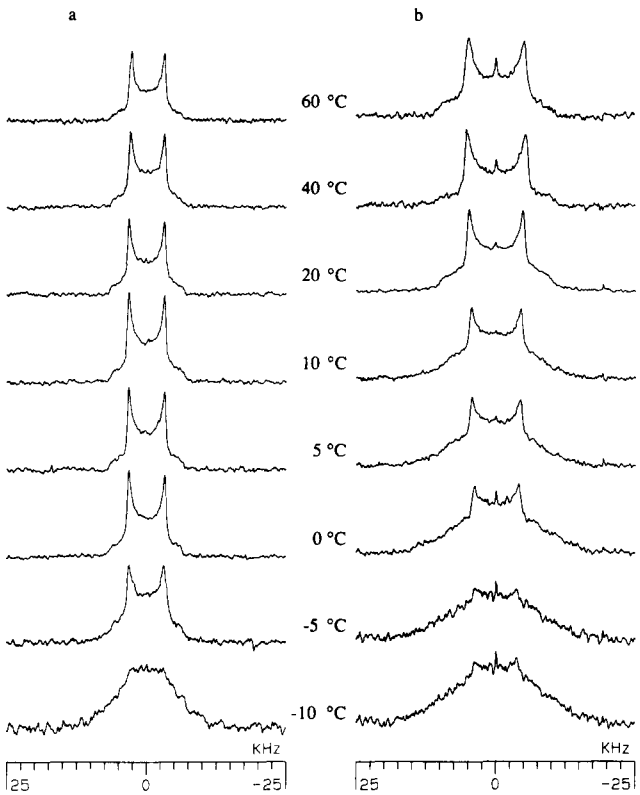

Fig. 3. Temperature dependence of the ^{2}H-NMR spectra from POPC-α-d_2 in membranes composed of: (a) 100% POPC; (b) POPC/DMPA in a 50:50 molar ratio. The temperatures are indicated.

most likely due to the presence of a minor population of small lipid vesicles. These are normally removed by centrifugation of the lipid sample. However, at high concentrations of DMPA the electrostatic repulsions increase the swelling of the bilayer and render centrifugation difficult.

Temperature dependence of the ^{2}H-NMR spectra

Fig. 3 compares the temperature dependence of the ^{2}H-NMR spectra from membranes composed of 100% POPC-α-d_2 (a) versus POPC-α-d_2 mixed with DMPA in a 50:50 molar ratio (b).

For the case of 100% POPC-α-d_2, at all temperatures above -5°C the spectra consist of an axially symmetric Pake pattern, indicative of a random dispersion of liquid-crystalline lipids in a bilayer arrangement [31]. With decreasing temperature the quadrupole splitting increases slightly, until at -5°C a second broad component appears in the NMR spectrum due to the onset of the gel/liquid-crystalline phase transition. At -10°C the phase transition is complete and the spectrum consists solely of the broad gel phase component.

The temperature dependence of the ^{2}H-NMR spectrum from the POPC-α-d_2/DMPA 50:50 mixture differs from that of 100% POPC-α-d_2 in two major respects. Firstly, the broad spectral component due to the gel phase lipid begins to appear at much higher temperatures, with its contribution to the overall spectrum increasing gradually over a wide temperature range. By -5°C the transition to the gel phase is complete and the ^{2}H-NMR spectrum consists entirely of the gel phase component. Secondly, the quadrupole splitting of the liquid-crystalline component decreases with decreasing temperature. Note that this latter behaviour is opposite to the temperature dependence of liquid-crystalline 100% POPC-α-d_2.

Fig. 4 compares the temperature dependence of the ^{2}H-NMR spectra from bilayers composed of 100% POPC-β-d_2 (a) versus POPC-β-d_2 mixed with DMPA in a 50:50 molar ratio (b).

For the case of 100% POPC-β-d_2, at all temperatures above -10°C, the ^{2}H-NMR spectrum consists of an axially symmetric Pake pattern. Decreasing the temperature brings about a gradual increase in the size of the quadrupole splitting, as observed for 100% POPC-α-d_2. However, even at -10°C there is little indication of the presence of gel phase lipid. In fact, the broad gel phase component only begins to appear at temperatures around -10°C. This failure to register the occurrence of the phase transition is not due to any difference in the thermotropic phase behaviour of POPC-α-

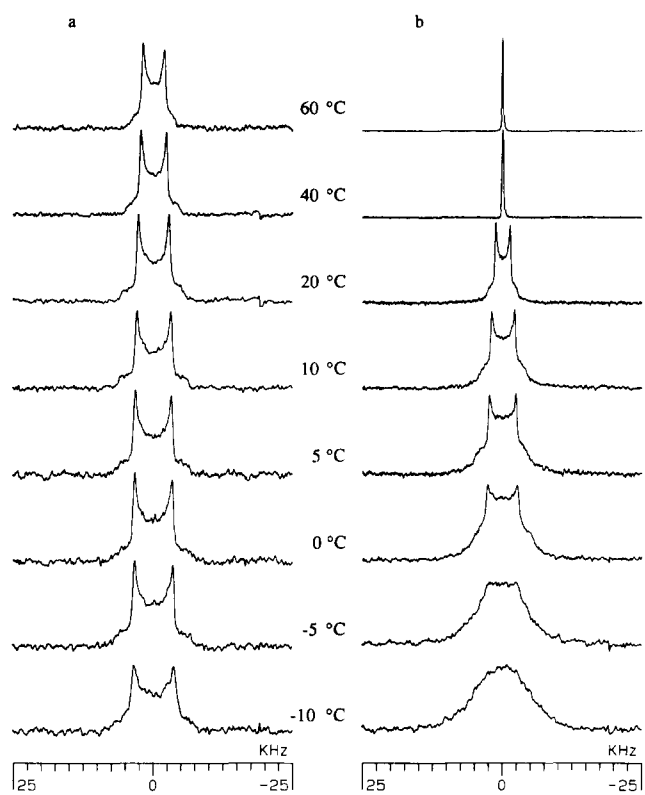

Fig. 4. Temperature dependence of the ^{2}H-NMR spectra from POPC-β-d_2 in membranes composed of: (a) 100% POPC; (b) POPC/DMPA in a 50:50 molar ratio. The temperatures are indicated.

d_2 versus POPC-α-d_2. Rather, it can be attributed to a greater mobility of the β-methylene segment of the choline headgroup compared to the α-methylene segment, which renders the line shape relatively insensitive to the onset of the phase transition.

The temperature dependence of the ^{2}H-NMR spectra from the POPC-β-d_2/DMPA 50:50 mixture is very different from that of 100% POPC-β-d_2. Firstly, as observed with the mixtures of POPC-α-d_2/DMPA, a broad spectral component attributable to gel phase lipid begins to appear at a temperature much higher than the phase transition temperature of 100% POPC. Its contribution to the overall spectral intensity gradually increases with decreasing temperature until at -5°C the transition to the gel state appears to be complete. Secondly, the quadrupole splitting of the liquid-crystalline component of the POPC-β-d_2/DMPA 50:50 mixture increases with decreasing temperature.

Comparison of Figs. 3b and 4b reveals that, for the POPC/DMPA 50:50 mixtures, there is little difference between the temperature dependence of the ^{2}H-NMR spectra from POPC-α-d_2 versus POPC-β-d_2 in terms of the proportions of the liquid-crystalline and gel phase spectral components. On the other hand, the temperature dependence of the $\Delta\nu$ measured from the liquid-crystalline phase component is completely different for POPC-α-d_2 versus POPC-β-d_2. The large counterdirectional change with decreasing temperature (α decreases; β increases) is again characteristic of a specific charge response of the POPC headgroup, but is opposite to the original change caused by the addition of anionic DMPA at 60°C. This indicates that decreasing the temperature produces a progressively lower negative surface charge in the liquid-crystalline phase. We interpret this effect as resulting from the lateral phase separation of DMPA-enriched gel phase domains which leaves the liquid-crystalline phase depleted in DMPA.

The ^{2}H-NMR spectra from mixtures of POPC and DMPA at intermediate temperatures appear to consist of a superposition of gel and liquid-crystalline phase components. This suggests the presence of coexisting gel and liquid-crystalline phase domains with only slow exchange of lipids (on the ^{2}H-NMR time scale). However, the distinction between a gel state ^{2}H-NMR spectrum and a liquid-crystalline state spectrum is not so unambiguous when the deuterons are located in the headgroup as when they are located elsewhere in the phospholipid molecule [32,33]. In order to demonstrate unambiguously that such ^{2}H-NMR spectra may be interpreted in terms of two separate components, one due to gel and the other due to liquid-crystalline lipids, we exploit the difference in the longitudinal (T_1) relaxation times of lipids present in thermotropic states so different in their characteristic molecular mobilities. Fig. 5 illustrates the ^{2}H-NMR spectra of POPC-β-d_2

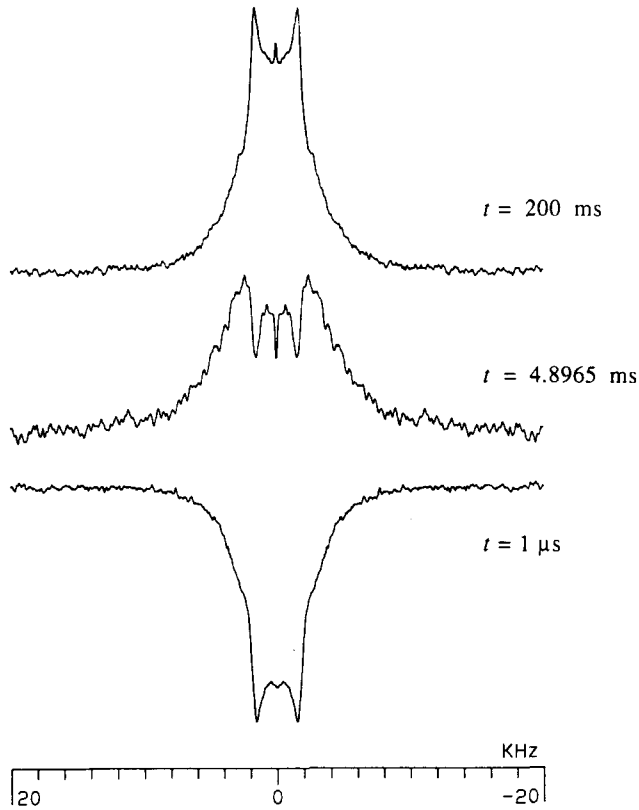

Fig. 5. T_1 inversion recovery spectra for POPC-β-d_2/DMPA in a 50:50 molar ratio at 15°C, obtained using three different inversion recovery delays (t). The upper spectrum was acquired with $t = 200$ ms and corresponds to complete recovery of the signal. The bottom spectrum with $t = 1$ μs, corresponds to full signal inversion. The middle spectrum was acquired with $t = 4.8965$ ms, a value intermediate between the inversion recovery t_{null} of the gel and liquid-crystalline spectral components.

mixed with 50 mol% DMPA, at 15°C, obtained with the combined inversion recovery-quadrupole echo pulse sequence (180_x-t-90_x-τ-90_y-τ-acq) using three different values of the post inversion delay, t. In the lower spectrum the delay following the 180° inversion pulse ($t = 1$ μs) is so short that the magnetization has no chance to relax towards its equilibrium value, and the spectrum is inverted. We estimate the longest T_1 relaxation time to be about 7 ms in this sample, at this temperature. In the upper spectrum the post inversion delay ($t = 200$ ms) is more than sufficient to permit the magnetization to return fully to its equilibrium value, and the spectrum has the usual orientation. In both the fully inverted and the fully relaxed spectra the liquid-crystalline and the gel phase spectral components behave identically. When the post inversion delay is carefully chosen ($t = 4.8965$ ms) such that it is intermediate between the t_{null} value (corresponding to $T_1 \cdot \ln 2$) of the faster relaxing component and that of the slower relaxing component, the spectrum is partially relaxed and consists of an inverted liquid-crystalline phase component together with an upright gel phase compo-

nent. The T_1 of the POPC headgroup deuterons is longer for liquid-crystalline than for gel phase lipids due to restricted motion in the latter. The results from the T_1 relaxation study of POPC-β-d_2 can be extrapolated to the case of POPC-α-d_2, and allow us to conclude that the ^{2}H-NMR line shapes observed at intermediate temperatures are indeed the result of two superimposed spectral components, one gel, the other liquid-crystalline.

Fig. 6 shows in detail how the quadrupole splitting of the liquid-crystalline component of the ^{2}H-NMR spectrum varies over the entire temperature range. For the sake of clarity only the results from representative POPC/DMPA mixtures are illustrated. Fig. 6a shows the data from POPC-α-d_2, while Fig. 6b shows the data from POPC-β-d_2 for corresponding mixtures with DMPA. For 100% POPC-α-d_2 and 100% POPC-β-d_2 the quadrupole splitting increases in a virtually linear fashion with decreasing temperature. The rate of change of the quadrupole splitting with changing temperature is greater for POPC-β-d_2 than for POPC-α-d_2. The temperature dependence of the POPC/DMPA mixtures, however, differs fundamentally from that of 100% POPC membranes in that each exhibits two abrupt changes in slope at characteristic temperatures. Note, for example, the case of the POPC-α-d_2/DMPA 80:20 mixture. Between 60°C and 20°C the quadrupole splitting increases in a linear fashion paralleling the behaviour of 100% POPC-α-d_2. However, below 20°C the quadrupole splitting suddenly begins to decrease with decreasing temperature, eventually reaching values typical of an electrically neutral 100% POPC-α-d_2 membrane. Similar behaviour is observed for all concentrations of DMPA, although differences in the details are apparent. Firstly, the high- and the low-temperature breaks move to progressively higher temperatures with increasing DMPA concentration. A second difference in detail is the size of the quadrupole splitting ultimately reached by the liquid-crystalline spectral component prior to complete conversion to the gel state. This too moves to higher values with increasing DMPA concentration. The high-temperature break in each of the temperature dependence curves approximately coincides with the first appearance of a gel phase component in the ^{2}H-NMR spectrum, and we associate it with the onset of gel phase domain growth in the bilayer membranes. The interpretation of the low-temperature break is more ambiguous and is discussed in the following section.

Turning to the case of the POPC-β-d_2/DMPA 80:20 mixture, it is evident that between 60°C and about 20°C the quadrupole splitting increases linearly in the same manner observed for 100% POPC-β-d_2 bilayers. However, below 20°C, the rate of increase of the quadrupole splitting with decreasing temperature accelerates, until at approx. 0°C the value of the quadrupole splitting approaches that of a neutral 100% POPC-β-d_2 bilayer. As was the case for the POPC-α-

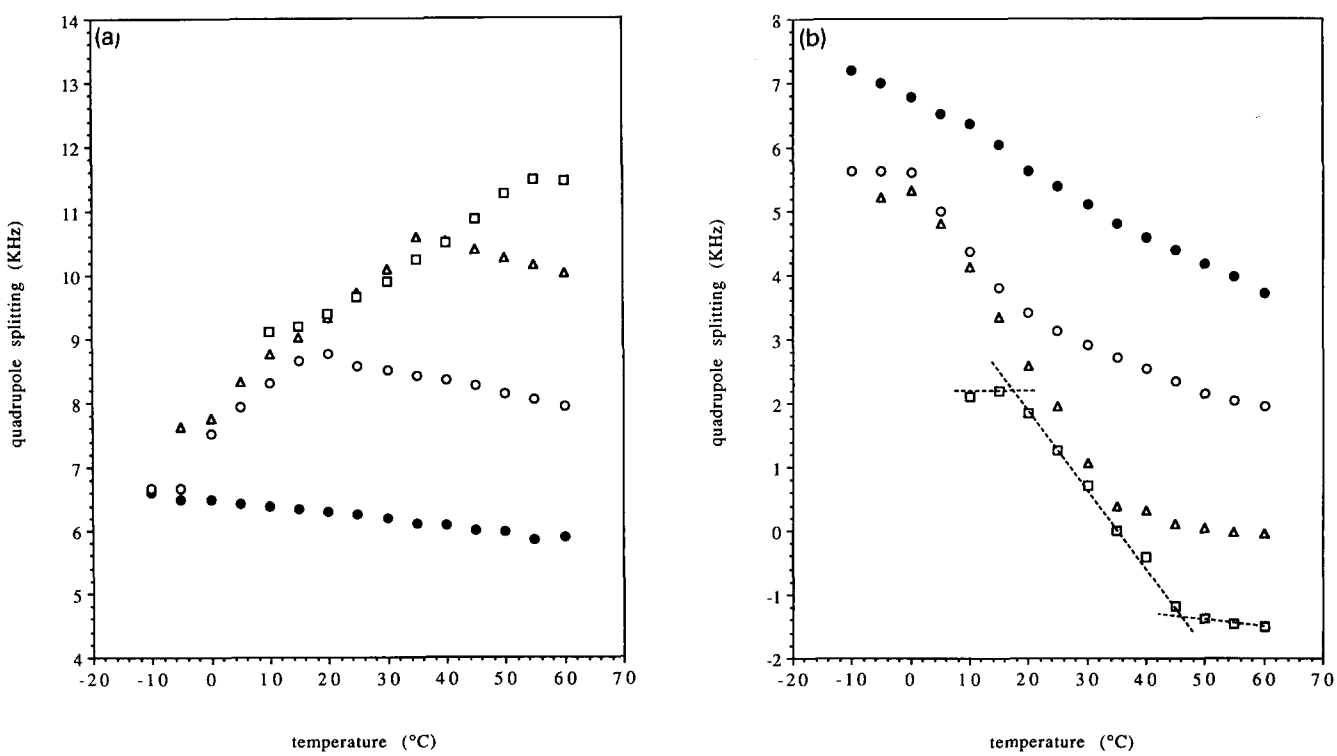

Fig. 6. ^{2}H-NMR quadrupole splittings plotted as a function of temperature for (a) POPC-α-d_2 and (b) POPC-β-d_2. (●) 0% DMPA; (○) 20 mol% DMPA; (△) 50 mol% DMPA; (□) 80 mol% DMPA.

d_2/DMPA mixtures, similar behaviour is apparent for all mixtures of POPC-β-d_2/DMPA. Again, the high- and low-temperature breaks at which the temperature dependence curve shifts its slope move to progressively higher temperature with increasing mole fraction of DMPA. Again, the value of the quadrupole splitting ultimately reached by the liquid-crystalline spectral component prior to complete conversion to the gel sate deviates more and more with increasing DMPA concentration from the value characteristic of a neutral 100% POPC-β-d_2 lipid bilayer. Moreover, the high temperature breaks again coincide with the temperatures at which a gel phase component is first observed in the ^{2}H-NMR spectrum of the POPC-β-d_2/DMPA mixtures and, therefore, must be associated with the onset of gel phase domain growth in the bilayer membranes.

Discussion

Our results demonstrate that surface charge distribution is a major determinant of the 'molecular voltmeter' response. In the following we show that the ^{2}H-NMR charge response of phosphocholine reflects the membrane surface charge distribution in a quantitative manner. This is demonstrated by constructing a phase diagram for the POPC/DMPA system which conforms with the behaviour expected from DSC. In addition, we discuss the implications of our findings for the application of the ^{2}H-NMR 'molecular voltmeter' to the study of electrostatic interactions between membrane proteins and lipids.

Phase diagram obtained from the ^{2}H-NMR charge response of POPC

In bilayers composed of binary mixtures of dissimilar phospholipids, lateral phase separation of solid domains of distinct composition is a well established phenomenon [34–36]. The miscibility profiles of such mixtures depend on the similarities in the chemicophysical properties of the component lipids, and are best characterized by means of a temperature versus concentration phase diagram. In the event of lateral separation of gel phase domains from the liquid-crystalline lipid pool, individual POPC molecules are no longer able to sample a distribution of charge environments representative of the global-average surface charge. In the gel phase rotational and translational diffusion are highly curtailed. Thus, the rate of exchange of lipids between gel and liquid-crystalline domains is slow on the ^{2}H-NMR time scale, and the two domains yield separate NMR signals. In the liquid-crystalline domains rapid rotational and translational diffusion still occurs and, therefore, the phosphatidylcholine molecules will report on the domain-average surface charge rather than on the global-average. In

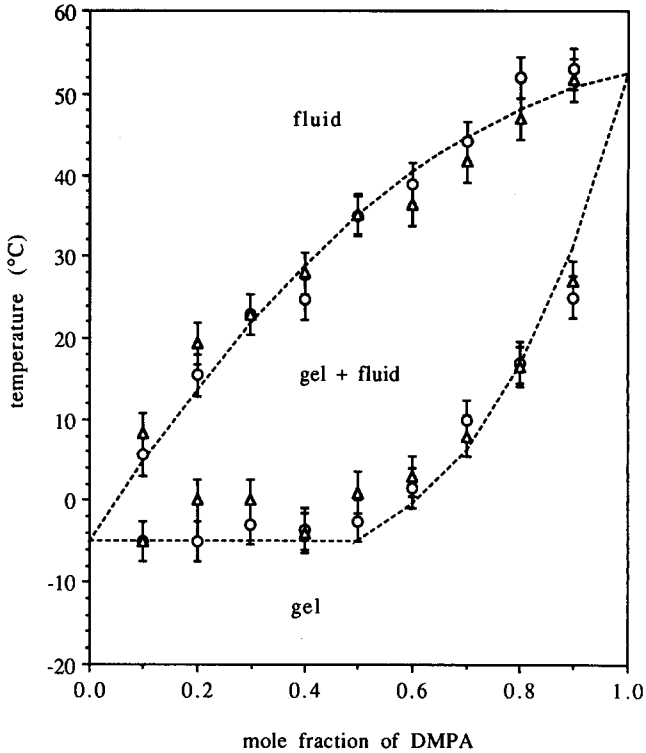

Fig. 7. Phase diagram for the POPC/DMPA system obtained from the high- and low-temperature breaks of the quadrupole splitting temperature dependence, T_f and T_s. (○) mixtures containing POPC-α-d_2; (△) mixtures containing POPC-β-d_2.

the situation reported here DMPA is the high melting phospholipid which becomes preferentially enriched in the gel phase domains. Simultaneously, the liquid-crystalline phase becomes depleted in DMPA and enriched in the lower melting phospholipid POPC. Effectively the POPC in the liquid-crystalline phase experiences a decreased domain-average surface charge relative to the global-average.

The generation of the POPC/DMPA phase diagram from the ^{2}H-NMR spectra of headgroup-deuterated POPC relies on our interpretation of the high- and low-temperature breaks in the temperature dependence profiles of the quadrupole splittings as corresponding to the onset and completion of lateral phase separation, respectively. In the quadrupole splitting temperature-dependence curves it is possible to draw straight lines through three distinct portions of each curve. The two points at which the lines intersect, T_f at high temperature and T_s at low temperature, are unique for each POPC/DMPA composition (see Fig. 6b). We interpret T_f as the onset of lateral phase separation. Plotting T_f against the net mole fraction of DMPA for the corresponding mixture yields the fluidus curve shown in Fig. 7. T_s is the temperature at which the steep portion of the quadrupole splitting temperature dependence curves level off. Below this temperature the size of the quadrupole splitting no longer

changes with decreasing temperature. This implies that below this temperature the composition of the liquid-crystalline phase should no longer change with further temperature decrease. Therefore, if we interpret T_s as the temperature at which lateral phase separation is complete, plotting T_s against the mole fraction of DMPA in its corresponding lipid mixture yields the curve shown in Fig. 7 which should correspond to the solidus curve of the phase diagram.

The results obtained from POPC-α-d_2 and from POPC-β-d_2 are essentially identical. Furthermore, the phase diagram shown in Fig. 7 is in good agreement with the DSC results. The fluidus curve in particular corresponds nicely with the upper temperature limits of the DSC endotherms. For the solidus curve, however, the correspondence is less favourable, due largely to the difficulty in measuring the quadrupole splitting from a small liquid-crystalline spectral component overlapping a large gel spectral component. A second important factor may be the following. The net surface charge experienced by a liquid-crystalline POPC molecule includes a contribution from the DMPA present in the liquid-crystalline phase, plus a contribution from gel phase DMPA at the gel phase domain boundaries. With decreasing temperature and increasing DMPA concentration, the total length of the gel phase domain boundary increases. At temperatures T_s, close to the solidus, the amount of DMPA remaining in the liquid-crystalline phase is very small. Therefore, the contribution to the negative surface charge from DMPA present at the gel phase domain boundary becomes more important, and the response of the quadrupole splitting to changes in the liquid-crystalline surface charge becomes less sensitive. Thus, the levelling off of the quadrupole splitting temperature dependence curve at T_s will not necessarily coincide with the completion of gel phase domain growth.

An alternate means of generating a partial POPC/DMPA phase diagram from the ^{2}H-NMR data involves focusing on the quadrupole splittings in the gel/liquid-crystalline coexistence region. Here the size of the quadrupole splitting at a particular temperature yields the DMPA composition of the liquid-crystalline component provided that a quadrupole splitting/composition calibration curve is available at that temperature. Such isothermal calibration curves can be generated if one assumes that the virtually linear temperature dependence of the quadrupole splitting observed in the 100% liquid-crystalline region (i.e., see Fig. 6) may be extrapolated to describe the temperature dependence of the liquid-crystalline component in the coexistence region. If each different initial POPC/DMPA composition is so treated, one may extract the expected dependence of the quadrupole splitting on the DMPA composition, at a particular temperature in the absence of lateral phase separation.

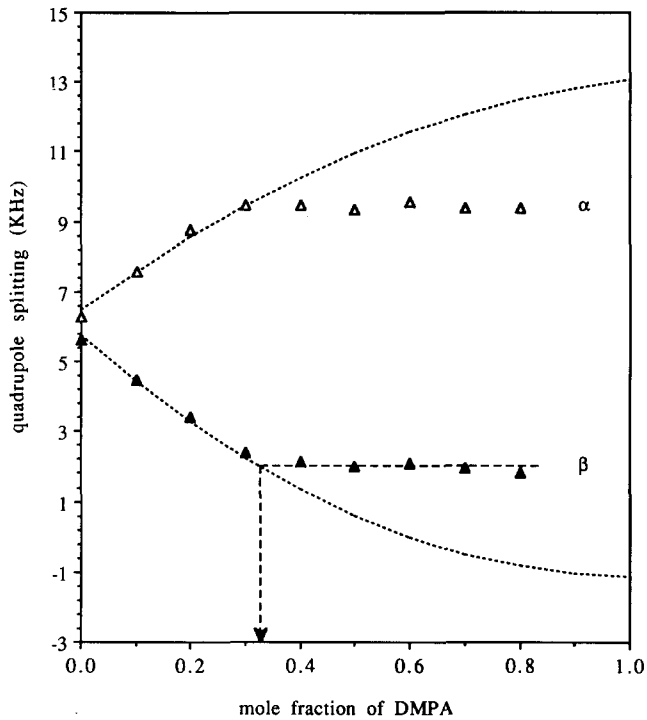

Fig. 8. Isothermal quadrupole splitting/DMPA composition calibration curves at 20°C (dotted line) obtained by using the linear extrapolation procedure described in the text. Also shown are the ^{2}H-NMR quadrupole splittings measured from POPC-α-d_2 (open symbols) and POPC-β-d_2 (closed symbols), at 20°C, plotted as a function of the initial DMPA concentration. The DMPA composition of the liquid-crystalline phase in the coexistence region is obtained by drawing a line horizontally from any one data point until it intersects the isothermal calibration curve, and then extrapolating down to intersect the DMPA composition axis.

Fig. 8 shows the isothermal calibration curves obtained at 20°C together with the measured quadrupole splittings. Deviations of the measured values from the extrapolated values above about 30 mol% DMPA indicate the presence of lateral phase separation of DMPA. The DMPA composition of the liquid-crystalline domains in the coexistence region may be read off from the isothermal calibration curve in the manner shown in the figure. Note that at 20°C the composition of the liquid-crystalline component in the coexistence region appears to be nearly identical for all values of the initial DMPA composition, and that identical results are obtained regardless of the deuterium label position in the choline headgroup.

The partial POPC/DMPA phase diagram which results from application of this method is shown in Fig. 9. Data from POPC-α-d_2 (circles) and POPC-β-d_2 (triangles) are shown separately. Each point represents the average DMPA composition at a given temperature and the error bars indicate the range of DMPA compositions. The fluidus curve determined in this fashion is virtually identical to that shown in Fig. 7. A particular uncertainty associated with this method involves the degree to which the quadrupole splitting of

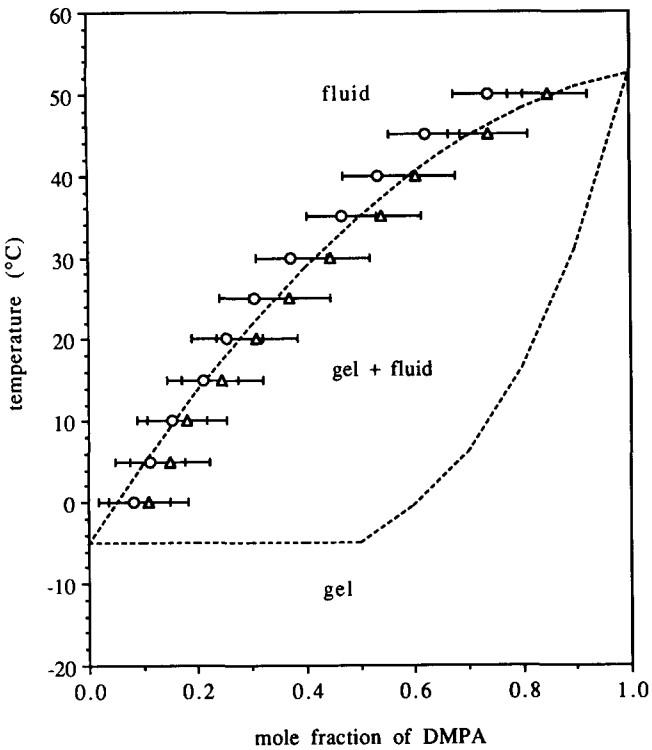

Fig. 9. Partial phase diagram for the POPC/DMPA system generated using the direct relationship between the quadrupole splittings from POPC-α-d_2 and POPC-β-d_2 and the concentration of DMPA. (○) mixtures containing POPC-α-d_2; (△) mixtures containing POPC-β-d_2. Each point represents the average DMPA composition at a given temperature and the error bars indicate the range of DMPA compositions. The dashed curve is the phase diagram obtained from the high- and low-temperature breaks of the quadrupole splitting temperature dependence as shown in Fig. 7.

liquid-crystalline POPC will be influenced by DMPA present at a gel phase domain boundary. Any such effect will be magnified at low-temperatures and high DMPA mole fraction and will lead to an apparently high DMPA content in the liquid-crystalline phase. Moreover, the magnitude of any such effect will reflect the size and morphology of the gel/liquid-crystalline domain boundaries and, hence, the morphology of the gel phase domains.

Finally, we note that the ^{2}H-NMR data provide yet a third means for generating the POPC/DMPA phase diagram. One may analyze the spectral line shape to determine the proportion of gel and liquid-crystalline phase components using the method of 'difference spectroscopy' described by Davis and co-workers [32,37–39]. This approach is elegant and powerful when applied to chain-deuterated lipids. However, the fact that in the present case the headgroup quadrupole splitting is a function of both temperature and surface charge density introduces additional and formidable complexities. Nevertheless, we point out that such an analysis of the ^{2}H-NMR spectra from chain-deuterated lipids combined with the approach described in this paper should provide a powerful method for mapping the phase diagrams of binary lipid mixtures containing phosphatidylcholine and a charged species. The former allows one to monitor lipid segmental order, while the latter allows one to monitor directly the composition of the liquid-crystalline phase.

Implications for the study of protein-lipid electrostatic interactions

In these experiments an inhomogeneous charge distribution has been induced thermally by exploiting the difference in the gel/liquid-crystalline phase transition temperatures of the two components. Electrostatic interactions between oppositely charged membrane components, such as proteins and lipids, constitute another possible means for achieving surface charge inhomogeneities in membranes. Several classes of proteins carry net positive charges and will bind preferentially to negatively charged lipids [40–45]. The issue is whether or not such electrostatic interactions are long-lived.

Recent ^{2}H-NMR studies [46] have demonstrated that in ternary mixtures of neutral, cationic and anionic lipids, under conditions of complete miscibility of all the membrane components, the charge response of phosphatidylcholine can be predicted from the individual responses of the corresponding binary mixtures of the species involved (neutral plus cationic and neutral plus anionic). In this case, if the electrostatic interactions between charged lipids and oppositely charged proteins are short-lived then the ^{2}H-NMR data will reflect the global-average surface charge, and it will be possible to predict the quadrupole splitting charge response from the individual responses of the corresponding binary mixtures. On the other hand, if lipid-protein electrostatic interactions lead to long-lived complexes then the ^{2}H-NMR data will report on a domain-average surface charge, and the observed charge response will reflect that of a binary mixture of phosphatidylcholine plus the charged species present in excess. Therefore, we conclude that the sensitivity of the 'molecular voltmeter' both to surface charge and to surface charge distribution provides a means to address this important biological issue.

Acknowledgement

The National Science and Engineering Research Council (NSERC) of Canada is acknowledged for support of this research.

References

1 Seelig, J., Macdonald, P.M. and Scherer, P.G. (1987) Biochemistry 26, 7535–7541.
2 Akutsu, H. and Seelig, J. (1981) Biochemistry 20, 7366–7373.

3 Roux, M., Neumann, J.M., Hodges, R.S., Devaux, P.F. and Bloom, M. (1989) Biochemistry 28, 2313–2321.
4 Scherer, P.G. and Seelig, J. (1989) Biochemistry 28, 7720–7728.
5 Macdonald, P.M., Leisen, J. and Marassi, F.M. (1991) Biochemistry 30, 3558–3566.
6 Altenbach, C. and Seelig, J. (1984) Biochemistry 23, 3913–3920.
7 Macdonald, P.M. and Seelig, J. (1987) Biochemistry 26, 6292–6298.
8 Macdonald, P.M. and Seelig, J. (1987) Biochemistry 26, 6769–6775.
9 Altenbach, C. and Seelig, J. (1985) Biochim. Biophys. Acta 818, 410–415.
10 Boulanger, Y., Schreier, S. and Smith, I.C.P. (1981) Biochemistry 20, 6824–6830.
11 Seelig, A., Allegrini, P.R. and Seelig, J. (1988) Biochim. Biophys. Acta 939, 267–276.
12 Beschiaschvili, G. and Seelig, J. (1990) Biochemistry 29, 52–58.
13 Dempsey, C., Bitbol, M. and Watts, A. (1989) Biochemistry 28, 6590–6596.
14 Hartsel, S.C. and Cafiso, D.S. (1986) Biochemistry 25, 8214–8219.
15 Winiski, A.P., McLaughlin, A.C., McDaniel, R.V., Eisenberg, M. and McLaughlin, S. (1986) Biochemistry 25, 8206–8214.
16 Lee, A.G. (1991) Progr. Lipid Res. 30, 323–348.
17 Lee, A.G. (1975) Progr. Biophys. Mol. Biol. 29, 3–56.
18 Lee, A.G. (1977) Biochim. Biophys. Acta 472, 285–344.
19 Cevc, G. and Marsh, D. (1987) Phospholipid Bilayers: Physical Principles and Models, Wiley, New York.
20 Gennis, R.B. (1989) Biomembranes: Molecular Structure and Function, Springer Verlag, New York.
21 De Kruiff, B., Demel, R.A., Slotboom, A.J., Van Deenen, L.L.M. and Rosenthal, A.F. (1973) Biochim. Biophys. Acta 307, 1–19.
22 Blume, A. (1983) Biochemistry 22, 5436–5442.
23 Graham, J., Gagné, J. and Silvius, J.R. (1985) Biochemistry 24, 7123–7131.
24 Harbisson, G.S. and Griffin, R.G. (1984) J. Lipid Res. 25, 1140–1142.
25 Aloy, M.M. and Rabaut, C. (1913) Bull. Soc. Chim. Fr. 13, 457–460.
26 Aneja, R., Chada, J.S. and Davies, A.P. (1970) Biochim. Biophys. Acta 218, 102–111.
27 Comfurius, P. and Zwaal, R.F.A. (1977) Biochim. Biophys. Acta 488, 36–42.
28 Davis, J.H., Jeffrey, K.R., Bloom, M., Valic, M.I. and Higgs, T.P. (1976) Chem. Phys. Lett. 42, 390–394.
29 Griffin, R.G. (1981) Methods Enzymol. 72, 108–174.
30 Sixl and Watts, A. (1983) Proc. Natl. Acad. Sci. USA 80, 1613–1615.
31 Seelig, J. (1977) Q. Rev. Biophys. 10, 353–418.
32 Vist, M.R. and Davis, J.H. (1990) Biochemistry 29, 451–464.
33 Davis, J.H. (1983) Biochim. Biophys. Acta 737, 117–171.
34 Shimshick, E.J. and McConnell, H.M. (1973) Biochemistry 12, 2351–2360.
35 Wu, S.H. and McConnell, H.M. (1975) Biochemistry 14, 847–854.
36 Lee, A.G. (1975) Biochim. Biophys. Acta 413, 11–23.
37 Huschilt, J.C., Hodges, R.S. and Davis, J.H. (1985) Biochemistry 24, 1377–1386.
38 Morrow, M.R., Huschilt, J.C. and Davis, J.H. (1985) Biochemistry 24, 5396–5406.
39 Morrow, M.R. and Davis, J.H. (1988) Biochemistry 27, 2024–2032.
40 Dufourcq, J. and Faucon, J.F. (1977) Biochim. Biophys. Acta 467, 1–11.
41 Op den Kamp, J.A.F. (1979) Annu. Rev. Biochem. 48, 47–71.
42 Batenburg, A.M., Van Esch, J.F., Verkleij, A.J., Leunissen-Bijvelt, J. and De Kruiff, B. (1987) FEBS Lett. 223, 148–154.
43 Bishop, R.W. and Bell, R.M. (1988) Annu. Rev. Cell Biol. 4, 479–610.
44 Mosior, M. and McLaughlin, S. (1992) Biochemistry 31, 1767–1773.
45 Keller, R.C.A., Killian, J.A. and De Kruiff, B. (1992) Biochemistry 31, 1672–1677.
46 Marassi, F.M. and Macdonald, P.M. (1992) Biochemistry 31, 10031–10036.